ACKNOWLEDGMENT

The author wishes to thank Dr. T. Hansen for his valuable comments on an earlier version of the manuscript and Prof. S. Pivnenko for [17]. Thanks are also extended to the two anonymous reviewers for their helpful suggestions.

REFERENCES

[1] A. D. Yaghjian, "An overview of near-field antenna measurements," *IEEE Trans Antenna Prop*, vol. 34, no. 12, pp. 435–445, Jul. 1986.
[2] J. Appel-Hansen, J. D. Dyson, and T. G. Hickman, "The Handbook of Antenna Design," in , A. W. Rudge, Ed. *et al.* London: Peter Peregrinus, 1986, vol. 1.
[3] M. G. Cote and R. M. Wing, "Demonstration of bistatic electromagnetic scattering measurements by spherical near-field scanning," in *Proc. AMTA Symp.*, 1993, p. 191.
[4] T. B. Hansen, R. A. Marr, U. H. W. Lammers, T. J. Tanigawa, and R. V. McGahan, "Bistatic RCS calculations from cylindrical near-field measurements–Part I: Theory," *IEEE Trans Antenna Propag.*, vol. 54, no. 12, pp. 3846–3856, Dec. 2006.
[5] R. A. Marr, U. H. W. Lammers, T. B. Hansen, T. J. Tanigawa, and R. V. McGahan, "Bistatic RCS calculations from cylindrical near-field measurements–Part II: Experiments," *IEEE Trans Antenna Propag.*, vol. 54, no. 12, pp. 3857–3864, Dec. 2006.
[6] B. J. Cown and C. E. Ryan Jr., "Near-field scattering measurements for determining complex target RCS," *IEEE Trans Antenna Propag.*, vol. 37, no. 5, pp. 576–585, May 1989.
[7] E. G. Farr, R. B. Rogers, G. R. Salo, and T. N. Truske, "Near-field bistatic RCS measurements" Rome Air Development Center, Tech. Rep., RADC-TR-89-198, Oct. 1989.
[8] D. Zahn and K. Sarabandi, "Near-field measurements of bistatic scattering from random rough surfaces," in *Proc. IEEE Antennas Propag. and URSI Symp.*, Salt Lake City, Utah, Jul. 2001, pp. 1730–1733.
[9] O. M. Bucci and G. Franceschetti, "On the degrees of freedom of scattered fields," *IEEE Trans Antenna Propag.*, vol. 37, no. 7, pp. 918–926, Jul. 1989.
[10] P. Petre and T. K. Sarkar, "Difference between modal expansion and integral equation methods for planar near-field to far-field transformation," *Progr. Electromagn. Res.*, vol. 12, pp. 37–56, 1996.
[11] F. D'Agostino, F. Ferrara, C. Gennarelli, R. Guerriero, and G. Riccio, "An effective technique for reducing the truncation error in the near-field-far-field trnasformation with plane-polar scanning," *Progr. Electromagn. Res.*, vol. 73, pp. 213–238, 1996.
[12] O. M. Bucci and M. D. Migliore, "A new method for avoiding the truncation error on near-field antenna measurements," *IEEE Trans Antenna Propag.*, vol. 54, no. 10, pp. 2940–2952, Oct. 2006.
[13] F. Ferrara, C. Gennarelli, R. Guerriero, G. Riccio, and C. Savarese, "Extrapolation of the outside near-field data in the cylindrical scanning," *Electromagnetics*, vol. 28, pp. 333–345, 2008.
[14] A. Papoulis, *Signal Analysis*. New York: McGraw-Hill, 1977.
[15] G. H. Golub and C. F. Van Loan, *Matrix Computations*, 3rd ed. Baltimore: The Johns Hopkins Univ. Press, 1996.
[16] G. T. Ruck, D. E. Barrick, W. D. Stuart, and C. K. Krichbaum, *Radar Cross Section Handbook*. New York: Plenum, 1970, vol. 1.
[17] S. Pivnenko, Private Communication, Oct. 2008.

Pitfalls in the Determination of Optical Cross Sections From Surface Integral Equation Simulations

Andreas M. Kern and Olivier J. F. Martin

***Abstract*—Calculation of electromagnetic cross sections from surface integral equation simulations, a popular approach in microwave studies and recently also in optics and plasmonics, requires only a single post-processing step, which can, however, be very sensitive to the precision of the simulation result. We investigate the accuracy and robustness of two methods for cross section calculation, displaying when and why errors may occur, in certain cases even unphysical behavior. A calculation recipe which avoids unphysical results is given, ensuring convergence of all obtained cross sections. This study will help judge the accuracy of performed simulations and can prevent misinterpretation of modeling results.**

***Index Terms*—Absorbing media, boundary element methods, integral equations, scattering.**

I. INTRODUCTION

Integral equation (IE) methods have proved especially suitable for electromagnetic scattering calculations as they require discretization only of the scatterer and not of the surrounding space while intrinsically supplying the field distribution in the scatterer's far field [1]–[9]. This far field information is particularly valuable when comparing simulations to experimental results. For example, the optical extinction cross section determined from a scattering simulation can be directly compared to optical transmission measurements, forming a direct link between simulation and experiment [10]. Similar approaches are taken at microwave and radio frequencies, where IE formulations are used to study radar cross section minimalization and radar absorbing materials [11]–[13]. We will see, however, that the post-processing steps used to calculate cross-sections in IE formulations can be extremely sensitive to small errors in the simulation results.

One IE formulation popular in optics is the volume integral equation (VIE) formulation [14]–[16] in which the scattered far field and the discretized volume elements' polarization can be used to accurately calculate scattering and absorption cross sections, and with these the extinction. Recently, we have shown the advantages of the transformation from a volume to a surface integral equation (SIE) formulation [17], many of which rely on the fact that only the surface of the scatterer need be discretized and not its whole volume. This, however, impedes absorption calculation as it is done in VIE methods.

In this paper, we study the applicability of two approaches for optical cross section calculation. Section II contains derivations of both approaches with reference but not restricted to the SIE method presented in [17]. In Section III we investigate the accuracy of these approaches when applied to a simple system, demonstrating under which conditions they produce correct results and when they fail.

Manuscript received August 25, 2009; revised November 12, 2009; accepted December 05, 2009. Date of publication March 29, 2010; date of current version June 03, 2010. This work was supported by the Swiss National Science Foundation (Grant No. 20021-116758).

The authors are with the Nanophotonics and Metrology Laboratory, Swiss Federal Institute of Technology Lausanne (EPFL), 1015 Lausanne, Switzerland (e-mail: andreas.kern@epfl.ch; olivier.martin@epfl.ch).

Digital Object Identifier 10.1109/TAP.2010.2046870

II. Calculation of Cross Sections

A. Poynting Vector (Method A)

An elegant way of calculating optical cross sections using a surface integral equation method is via the Poynting vector of the electromagnetic field outside the scatterer. Consider a scatterer Ω completely enclosed by an arbitrary surface A. As the time-averaged Poynting vector,

$$\mathbf{S}(\mathbf{r}) = \frac{1}{2}\mathrm{Re}\left\{\mathbf{E}(\mathbf{r}) \times \mathbf{H}^*(\mathbf{r})\right\} \tag{1}$$

represents the energy flux density of an electromagnetic field, its integral over A,

$$\int_A \mathrm{d}\mathbf{A} \cdot \mathbf{S}(\mathbf{r}) = -P_{\mathrm{abs}} \tag{2}$$

is the power generated inside of A or, equivalently, the negative of the power absorbed. If we assume the space surrounding the scatterer to be non-lossy, this absorption can only occur inside the scatterer. The absorption cross section of the scatterer can then be easily calculated using the relation

$$C_{\mathrm{abs}} = \frac{P_{\mathrm{abs}}}{I_i} \tag{3}$$

where I_i is the incident intensity. For plane wave illumination $I_i = |\mathbf{E}_i|^2/(2Z_0)$, where $Z_0 = (\mu_0/\epsilon_0)^{1/2}$ is the free-space impedance.

Other optical cross sections can be computed if one rewrites the field outside the scatterer [18] as

$$\mathbf{E}(\mathbf{r}) = \mathbf{E}_i(\mathbf{r}) + \mathbf{E}_s(\mathbf{r}), \quad \mathbf{H}(\mathbf{r}) = \mathbf{H}_i(\mathbf{r}) + \mathbf{H}_s(\mathbf{r}) \tag{4}$$

where $\mathbf{E}_s, \mathbf{H}_s$ are the scattered electric and magnetic fields and $\mathbf{E}_i, \mathbf{H}_i$ are the incident fields without the scatter. These separate fields are in fact the output of most surface integral equation formulations but can also be obtained by simple arithmetic given the total and incident fields if needed. Inserting (4) into (1), the Poynting vector outside the particle can be written as

$$\mathbf{S}(\mathbf{r}) = \mathbf{S}_{\mathrm{inc}}(\mathbf{r}) + \mathbf{S}_{\mathrm{sca}}(\mathbf{r}) + \mathbf{S}_{\mathrm{ext}}(\mathbf{r}) \tag{5}$$

with

$$\mathbf{S}_{\mathrm{inc}}(\mathbf{r}) = \frac{1}{2}\mathrm{Re}\left\{\mathbf{E}_i(\mathbf{r}) \times \mathbf{H}_i^*(\mathbf{r})\right\}, \tag{6a}$$

$$\mathbf{S}_{\mathrm{sca}}(\mathbf{r}) = \frac{1}{2}\mathrm{Re}\left\{\mathbf{E}_s(\mathbf{r}) \times \mathbf{H}_s^*(\mathbf{r})\right\}, \tag{6b}$$

$$\mathbf{S}_{\mathrm{ext}}(\mathbf{r}) = \frac{1}{2}\mathrm{Re}\left\{\mathbf{E}_s(\mathbf{r}) \times \mathbf{H}_i^*(\mathbf{r}) + \mathbf{E}_i(\mathbf{r}) \times \mathbf{H}_s^*(\mathbf{r})\right\}. \tag{6c}$$

Integrating (5) over A, we obtain the optical energy conservation law,

$$P_{\mathrm{abs}} = P_{\mathrm{ext}} - P_{\mathrm{sca}} \tag{7}$$

where

$$P_{\mathrm{sca}} = \int_A \mathrm{d}\mathbf{A} \cdot \mathbf{S}_{\mathrm{sca}}(\mathbf{r}), \tag{8a}$$

$$P_{\mathrm{ext}} = -\int_A \mathrm{d}\mathbf{A} \cdot \mathbf{S}_{\mathrm{ext}}(\mathbf{r}). \tag{8b}$$

As the background without the scatterer is non-lossy, the integral over $\mathbf{S}_{\mathrm{inc}}$ is zero. Equations (8a) and (8b) can be solved numerically, e.g. by Gaussian quadrature [19], and the scattering and extinction cross sections, respectively, determined analogously to (3).

1) Reference to SIE Approach: When using an approach similar to the SIE formulation presented in [17], the absorption cross section can be directly and very conveniently computed without further discretization or numerical integration using the scatterer's surface itself as the integration surface A. The result of the method presented in [17] is the distribution of the electric and magnetic surface currents, $\mathbf{J}(\mathbf{r})$ and $\mathbf{M}(\mathbf{r})$, respectively, defined as

$$\mathbf{J}(\mathbf{r}) = \hat{\mathbf{n}}(\mathbf{r}) \times \mathbf{H}(\mathbf{r}), \quad \mathbf{M}(\mathbf{r}) = -\hat{\mathbf{n}}(\mathbf{r}) \times \mathbf{E}(\mathbf{r}) \tag{9}$$

for $\mathbf{r}$ on the scatterer's surface S, see Sec. 2.A. in [17]. Here, $\hat{\mathbf{n}}$ is the outward facing normal vector on S. One can rewrite (2) in terms of these surface currents using the relation

$$\begin{aligned}\hat{\mathbf{n}} \cdot (\mathbf{E} \times \mathbf{H}^*) &= (\hat{\mathbf{n}} \times \mathbf{E}) \cdot \mathbf{H}^* \\ &= -\mathbf{M} \cdot \mathbf{H}^* \\ &= -\mathbf{M} \cdot \mathbf{H}_{\tan}^* \\ &= \mathbf{M} \cdot (\hat{\mathbf{n}} \times \mathbf{J}^*) = \hat{\mathbf{n}} \cdot (\mathbf{J}^* \times \mathbf{M}),\end{aligned} \tag{10}$$

where the subscript tan denotes tangential components. Here we have used the fact that $\mathbf{J}$ and $\mathbf{M}$ only contain components tangential to the surface. In general, the surface currents are expanded in terms of easily integrated basis functions and (2) can be numerically solved simply by summing over the expansion coefficients (α_n, β_n in [17]).

B. Ohmic Loss (Method B)

A demonstrative way of calculating the absorption of a scatterer is by calculating its Ohmic loss. In most simulations, the physical properties of the scatterer are given by its complex index of refraction n or complex dielectric function $\epsilon_r \equiv \epsilon/\epsilon_0 = n^2$ (nonmagnetic scatterers assumed throughout this paper). Rewriting Ampère's law for time-harmonic fields to let a current density $\mathbf{j} = \sigma\mathbf{E}$ describe the effect of a medium, an expression for the complex conductivity can be derived,

$$\sigma = -i\omega\epsilon_0(\epsilon_r - 1). \tag{11}$$

The Ohmic loss in a scatterer Ω of conductivity σ in the time-harmonic electric field $\mathbf{E}$ is given by

$$P_{\mathrm{Ohm}} = \frac{1}{2}\int_\Omega \mathrm{d}V \mathrm{Re}\{\sigma\}\left|\mathbf{E}(\mathbf{r})\right|^2. \tag{12}$$

P_{Ohm} is the power removed from the electromagnetic field, thus the power absorbed by the scatterer. Consequently, we can use it to determine the absorption cross section of the scatterer analogously to (3).

III. Implementation Accuracy

Though the presented methods are mathematically exact, when implemented in numerical schemes they may show considerable errors in certain situations. In this section, the origins and occurrence of these errors will be investigated.

To be able to determine the error of a computed cross section, a system was chosen for which an exact solution can be derived. Cross sections were determined for a silver sphere of radius $r_{\mathrm{sph}} = 60\ \mathrm{nm}$ and compared with those obtained with the Mie solution [18], [20]. The relative dielectric function $\epsilon_r(\omega)$ of silver was taken from [21] and simulations were performed using an SIE/PMCHWT [17], [22]–[24] formulation, suited for high-permittivity scatterers of arbitrary shape.

The obtained optical cross sections divided by the physical cross section of the sphere $C_{\mathrm{sph}} = \pi r_{\mathrm{sph}}^2$ are shown in Fig. 1(a)–(c). Fig. 1(d) is the absolute value of the deviation of the simulated absorption cross

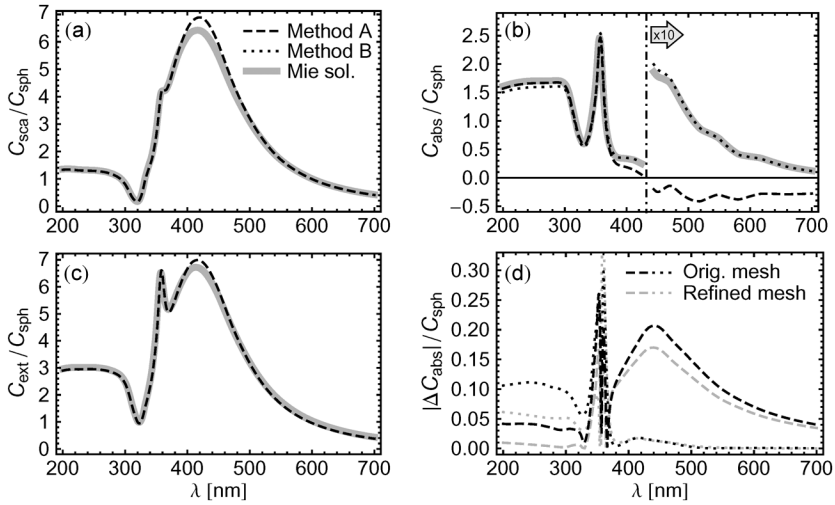

Fig. 1. Scattering, absorption and extinction cross sections [(a), (b) and (c), respectively] of a silver sphere ($r_{\mathrm{sph}} = 60\ \mathrm{nm}$) obtained by Poynting vector integration (method A) and Ohmic loss (method B) compared to the exact Mie solution. Curves in (b) are magnified x10 to the right of the dash-dotted line. Note that scattering and extinction cross sections cannot be determined using method B alone. The absolute value of the error of the absorption cross section calculated using Methods A and B is shown in (d) for original (used for (a)–(c)) and refined simulation meshes (see text).

sections from the Mie solution. One can see that the simulated scattering and extinction spectra are in good agreement with the exact solutions while the absorption cross section shows a considerable error especially for small absolute values. Particularly disquieting is the negative absorption cross section obtained by method A for $\lambda > 430\ \mathrm{nm}$.

This error as well as its absence using method B can be explained by both methods' numerical calculation: Method A is computed using (2) while method B is determined using (12). In the simple case of first-order Gaussian quadrature, these integrals can be written as sums,

$$C_{\mathrm{abs}}^{A} = -\frac{1}{I_i}\sum_n A_n \hat{\mathbf{n}}_n \cdot \mathbf{S}(\mathbf{r}_n) \tag{13a}$$

$$C_{\mathrm{abs}}^{B} = \frac{1}{I_i}\sum_n \frac{1}{2} V_n \mathrm{Re}\{\sigma\}\,|\mathbf{E}(\mathbf{r}_n)|^2 \tag{13b}$$

where A_n and $\hat{\mathbf{n}}_n$ are the areas and oriented normal vectors of the discretized surface elements of A, V_n are the volumes of the discretized volume elements of Ω and $\mathbf{r}_n$ are the respective element centroids. Note that (13b) requires additional discretization of the scatterer's volume, as further discussed at the end of this section. One can see that the summands in (13a) can be either negative or positive, their absolute value can thus be much larger than the total sum if canceled out by a similarly large summand of opposite sign. The summands in (13b), on the other hand, can only be positive and must thus be smaller than the total sum.

For the above example, the surface A was chosen as the surface of a sphere of radius $r_A = 500\ \mathrm{nm}$. The method presented in Section II-A-1 was not used here in order to extend the applicability of this study to a wider range of simulation techniques. Equations (2) and (12) were computed using first-order Gaussian quadrature, dividing surface A into $N_A = 9026$ triangles for method A and the scatterer into $N_B = 2848$ tetrahedra for method B. In both cases, the integration precision was chosen so that no improvement could be perceived in Fig. 1 upon further refinement. In our calculations, the absolute value of the summands in (13a) was on average 435 times larger than those in (13b), for low absorption ($\lambda = 600\ \mathrm{nm}$) even 1185 times.

If we concede that the summands in both (13a) and (13b) contain the product of two fields, we can say in rough approximation that the relative errors of both summands should be similar if the relative errors of the fields are the same. Noting that (13a) requires the field outside and (13b) the field inside of the scatterer, we must now differentiate between two cases as follows.

1) Strong scattering where $E_s \gg E_i$ and $H_s \gg H_i$. In this case, $\mathbf{E}$ inside and outside the scatterer is dominated by $\mathbf{E}_s$ and is afflicted with the full error of $\mathbf{E}_s$. Consequently, we can assume summands in both (13a) and (13b) to have the same relative error but as the absolute values of the summands in (13b) are considerably smaller, so will the total error in method B.
2) Weak scattering where $E_s \approx E_i$ and $H_s \approx H_i$. In this case, $\mathbf{E}$ outside the scatterer is no longer dominated by $\mathbf{E}_s$ and its error can be assumed to be smaller, as $\mathbf{E}_i$ is assumed to be exact. Inside the scatterer, $\mathbf{E} = \mathbf{E}_s$ is still valid (see Eq. (35) in [17]) and $\mathbf{E}$ is afflicted with the full error of $\mathbf{E}_s$. The summands in (13a) now have smaller relative errors than those in (13b) and the total error using method A may be equal to or less than that obtained using method B.

A typical setting for case 1 in the given spectra is at 450 nm. Here, scattering is strong and absorption is weak, thus the error in the absorption cross section is large when using method A. The area around 250 nm represents a typical setting for case 2 with weak scattering of the same order as the absorption. Here the error in the absorption cross section is smaller using method A than using method B.

As the error of the summands in (13a) depends on the scattering strength, one might assume the error of the absorption cross section using method A to correlate with the scattering cross section. Indeed, with the exception of the absorption peak at $\lambda \approx 360\ \mathrm{nm}$, the dashed curves in Figs. 1(a) and (d) show strong resemblance. Also, as the relative error of the summands in (13b) remains constant, one would assume the absorption cross section obtained using method B to have a constant relative error. Again one can see a strong resemblance between the dotted curves in Fig. 1(b) and (d). This becomes an advantage in the higher wavelength region as the absorption diminishes: though the scattering is fairly weak, method A produces a large relative error in the absorption cross section despite a moderate absolute error. Another advantage of method B is the fact that it cannot result in unphysical negative absorption values as is the case with method A.

As the cross sections in Fig. 1 contain errors of the simulation process as well as the post-processing methods, a second simulation was run with increased numerical precision to assess the influence of

this error source. By refining the simulation mesh by a factor of three, the average RMS error of the simulation output (surface currents $\mathbf{J}$ and $\mathbf{M}$) over the given spectrum was reduced by one third (from 6.6% to 4.5%) at the cost of 9 times the memory requirement. The errors of the thus obtained cross sections are shown in Fig. 1(d) in gray, their averages dropping by 25% and 36% for methods A and B, respectively. This shows that the error of the outputs of both, methods A and B, can be reduced by improving the accuracy of the underlying simulation. However, in particular for low absorption, unrealistic computational demands would be set for method A to reach the precision obtained using method B.

While method B seems to be the more reliable of the two approaches, offering at the least a predictable error, it is burdened by the need to discretize the volume of the scatterer for numerical integration. If a detailed geometric description of the scatterer is known, this can be done by volume meshing software with subsequent Gaussian quadrature. Alternately, if only the surface mesh as required by the SIE simulation is given, a more statistical approach may be followed using Monte-Carlo integration [25], in which N points are randomly distributed within a volume V completely containing the scatterer. Using a binary space partitioning (BSP) tree [26], one can quickly determine if a given point is inside or outside of the surface mesh. Summing over all the points inside the scatterer multiplied by V/N then gives an approximation of the integral.

IV. Conclusion

We have compared two methods for determining optical cross sections of isolated scatterers. Method A, via Poynting vector integration, is especially suitable for surface integral equation formulations as it requires no further discretization of the scatterer. In addition, scattering and extinction as well as absorption cross sections can be determined using this method. Also, the absorption cross section can be computed very efficiently via this method when using an SIE formulation, requiring no further numerical integration. Method B, via Ohmic loss in the scatterer, is only capable of supplying the absorption cross section, but with a low and predictable error. This method, however, requires volume discretization of the scatterer.

We have shown that the absorption cross section determined using method A shows large errors in situations with strong scattering. Also, if the absorption is weak, method A may produce unphysical negative absorption. These effects as well as their absence using method B can be explained if one considers the numerical implementation of both methods.

A robust procedure for determining all three optical cross sections would thus be to determine the scattering cross section using method A, the absorption cross section using method B and the extinction cross section using (7). This combination ensures good convergence of all cross sections and avoids the unphysical case of negative absorption. It should be noted that while the examples given in this paper were taken from optics, the presented methods are valid also at longer wavelengths and can easily be applied to microwave and radio frequency cross section calculations.

References

[1] M. Nieto-Vesperinas, *Scattering and Diffraction in Physical Optics*, 2nd ed. Singapore: World Scientific, 2006.

[2] W.-H. Y. Yang, G. C. Schatz, and R. P. Van Duyne, "Discrete dipole approximation for calculating extinction and Raman intensities for small particles with arbitrary shapes," *J. Comput. Phys.*, vol. 103, no. 3, pp. 869–875, 1995.

[3] R. D. Averitt, S. L. Westcott, and N. J. Halas, "Linear optical properties of gold nanoshells," *J. Opt. Soc. Am. B*, vol. 16, no. 10, pp. 1824–1832, 1999.

[4] E. Hao, S. Li, R. C. Bailey, S. Zou, G. C. Schatz, and J. T. Hupp, "Optical properties of metal nanoshells," *J. Phys. Chem. B*, vol. 108, no. 4, pp. 1224–1229, 2004.

[5] P. J. Valle, F. Moreno, and J. M. Saiz, "Comparison of real- and perfect-conductor approaches for scattering by a cylinder on a flat substrate," *J. Opt. Soc. Am. A*, vol. 15, no. 1, p. 158, 1998.

[6] Y.-H. Chu and W. C. Chew, "Large-scale computation for electrically small structures using surface-integral equation method," *Microwave Opt. Tech. Lett.*, vol. 47, no. 6, pp. 525–530, 2005.

[7] J. Jung and T. Sondergaard, "Green's function surface integral equation method for theoretical analysis of scatterers close to a metal interface," *Phys. Rev. B*, vol. 77, no. 24, p. 245310, 2008.

[8] I. Romero, J. Aizpurua, G. W. Bryant, and F. J. García de Abajo, "Plasmons in nearly touching metallic nanoparticles: Singular response in the limit of touching dimers," *Opt. Express*, vol. 14, no. 21, pp. 9988–9999, 2006.

[9] A. F. Peterson, R. Mittra, and S. L. Ray, *Computational Methods for Electromagnetics*. Piscataway, NJ: IEEE Press, 1998.

[10] T. R. Jensen, G. C. Schatz, and R. P. Van Duyne, "Nanosphere lithography: Surface plasmon resonance spectrum of a periodic array of silver nanoparticles by ultraviolet-visible extinction spectroscopy and electrodynamic modeling," *J. Phys. Chem. B*, vol. 103, no. 13, pp. 2394–2401, 1999.

[11] H. Strifors and G. Gaunaurd, "Scattering of electromagnetic pulses by simple-shaped targets with radar cross section modified by a dielectric coating," *IEEE Trans. Antennas Propag.*, vol. 46, no. 9, pp. 1252–1262, 1998.

[12] Y. M. M. Antar and H. Liu, "Effect of radar-absorbing materials on RCS of partially coated targets," *Microw. Opt. Techn. Lett.*, vol. 17, no. 5, pp. 281–284, 1998.

[13] H. Mosallaei and Y. Rahmat-Samii, "RCS reduction of canonical targets using genetic algorithm synthesized RAM," *IEEE Trans. Antennas Propag.*, vol. 48, no. 10, pp. 1594–1606, 2000.

[14] B. T. Draine, "The discrete-dipole approximation and its application to interstellar graphite grains," *Astrophys. J.*, vol. 333, pp. 848–872, 1988.

[15] B. T. Draine and P. J. Flatau, "Discrete-dipole approximation for scattering calculations," *J. Opt. Soc. Am. A*, vol. 11, no. 4, pp. 1491–1499, 1994.

[16] O. J. F. Martin and N. B. Piller, "Electromagnetic scattering in polarizable backgrounds," *Phys. Rev. E*, vol. 58, no. 3, pp. 3909–3915, 1998.

[17] A. M. Kern and O. J. F. Martin, "Surface integral formulation for 3D simulations of plasmonic and high permittivity nanostructures," *J. Opt. Soc. Am. A*, vol. 26, no. 4, pp. 732–740, 2009.

[18] C. Bohren and D. Huffmann, *Absorption and Scattering of Light by Small Particles*. New York: Wiley, 1983.

[19] G. R. Cowper, "Gaussian quadrature formulas for triangles," *Int. J. Numer. Methods Eng.*, vol. 7, no. 3, pp. 405–408, 1973.

[20] G. Mie, "Beiträge zur Optik trüber Medien, speziell kolloidaler Metallösungen," *Ann. Phys.*, vol. 25, no. 3, pp. 377–445, 1908.

[21] P. B. Johnson and R. W. Christy, "Optical constants of the noble metals," *Phys. Rev. B*, vol. 6, no. 12, pp. 4370–4379, 1972.

[22] A. J. Poggio and E. K. Miller, "Integral equation solutions of three dimensional scattering problems," in *Computer Techniques for Electromagnetics*. Oxford, U.K.: Permagon, 1973.

[23] Y. Chang and R. Harrington, "A surface formulation for characteristic modes of material bodies," *IEEE Trans. Antennas Propag.*, vol. 25, no. 6, pp. 789–795, 1977.

[24] T.-K. Wu and L. L. Tsai, "Scattering from arbitrarily-shaped lossy dielectric bodies of revolution," *Radio Sci.*, vol. 12, pp. 709–718, 1977.

[25] R. E. Caflisch, "Monte Carlo and quasi-Monte Carlo methods," *Acta Numerica*, vol. 7, pp. 1–49, 1998.

[26] M. S. Paterson and F. F. Yao, "Efficient binary space partitions for hidden-surface removal and solid modeling," *Discrete Comput. Geom.*, vol. 5, no. 1, pp. 485–503, 1990.